Geoscience Frontiers 15 (2024) 101699

Contents lists available at ScienceDirect

Geoscience Frontiers

journal homepage: www.elsevier.com/locate/gsf

Research Paper

Fe-Mn interdiffusion in aluminosilicate garnets

Yanjun Yin [a,b], Baohua Zhang [c,*], Xinzhuan Guo [a]

[a] Key Laboratory of High-temperature and High-pressure Study of the Earth's Interior, Institute of Geochemistry, Chinese Academy of Sciences, Guiyang 550081, Guizhou, China
[b] University of Chinese Academy of Sciences, Beijing 100049, China
[c] Key Laboratory of Big Data in Geosciences and Deep Earth Resources of Zhejiang Province, School of Earth Sciences, Zhejiang University, Hangzhou 310058, China

ARTICLE INFO

Article history:
Received 13 March 2023
Revised 20 August 2023
Accepted 22 August 2023
Available online 28 August 2023
Handling Editor: Richard Palin

Keywords:
Fe-Mn interdiffusion
Diffusion coefficient
Garnet
High pressure experiment
Water

ABSTRACT

Precise determination of cation diffusivity in garnet can provide critical information for quantitatively understanding the timescales and thermodynamics of various geological processes, but very few studies have been performed for Fe-Mn interdiffusion. In this study, Fe-Mn interdiffusion rates in natural single crystals of Mn-bearing garnet with 750 ppm H_2O are determined at 6 GPa and 1273–1573 K in a Kawai-type multi-anvil apparatus. Diffusion profiles were acquired by electron microprobe and fitted using Boltzmann–Matano equation. The experimental results show that the Fe-Mn interdiffusion coefficient ($D_{Fe\text{-}Mn}$) slightly decreases with increasing X_{Fe}. The experimentally determined $D_{Fe\text{-}Mn}$ in Mn-bearing garnet can be fitted by the Arrhenius equation: $D_{Fe-Mn}(m^2/s) = D_0 X_{Fe}^n \exp(-E^*/RT)$, where $E^* = (1 - X_{Fe})E^*_{Mn} + X_{Fe}E^*_{Fe}$, $D_0 = 8.06^{+9.87}_{-6.04} \times 10^{-9}$ m^2/s, $E^*_{Mn} = 248 \pm 27$ kJ/mol, $E^*_{Fe} = 226 \pm 59$ kJ/mol, $n = -1.36 \pm 0.51$. The comparing the present results with previous experimental data suggest that water can greatly enhance the $D_{Fe\text{-}Mn}$ in garnet. Our results indicate that the time required for homogenization of the compositional zoning of a garnet is much shorter than previously thought.

1. Introduction

Garnet is an important rock-forming mineral, which is found in diverse igneous and metamorphic rocks in the Earth's crust and mantle. Since diffusion in garnet is isotropic stemming from its isometric symmetry property, diverse compositional zonings of both divalent and trivalent cations are shown in natural samples (Chakraborty and Ganguly, 1991, 1992), which provide valuable windows for disclosing thermal and chemical histories of hosting rocks. Therefore, precise determination of cation diffusivity in garnet is crucial for understanding the timescales and thermodynamics of various geological processes such as cooling rates, exhumation rates, and the pressure–temperature (*P-T*) paths of the host rocks (Ganguly et al., 1998, 2000; Ganguly, 2002; Perchuk et al., 2008; Baxter and Scherer, 2013; Zhang, 2017; Li et al., 2018).

Given the presence of multicomponent in aluminosilicate garnet and the unavailability of suitable crystals to separate diffusion of one specific cation from another, experimental measurement of cation (i.e., Fe-Mn/Mg, Ca and Mn) diffusion is necessary to adequately cover the wide compositional space. Despite manganese (Mn) being a minor element in garnets, with concentrations ranging from 0.2 wt.% to 0.7 wt.% in peridotite garnets (Creighton, 2009), Mn plays a significant role in compositional zoning of garnet. Mn and Fe commonly exist together, resulting in conspicuous complementary zoning profiles in the growth zoning of garnet, where the Mn content typically decreases from the center to the edge while the Fe content increases. The Fe-Mn interdiffusion, which is one of the most important diffusion exchanges in garnet, would contribute to relax the growth-induced zoning at high temperature (Loomis, 1983). Applying the Fe-Mn interdiffusion to compositional zoning in garnet would deduce the timescales and thermodynamics of various geological processes mentioned above. Previous studies on natural aluminosilicate garnets have demonstrated that the diffusion of divalent cations varies according to their compositions (Elphick et al., 1985; Chakraborty and Ganguly, 1992; Perchuk et al., 2008). For example, Fe diffusivity (D_{Fe}) is almost identical to that of Mg (D_{Mg}) in Fe-poor and Mn-rich garnets, whereas D_{Fe} is lower than D_{Mg} in Fe-Mg-rich garnets (Loomis et al., 1985; Ganguly et al., 1998). However, the compositional dependence of the Fe-Mn interdiffusion in garnet remains controversial. To address this issue, we present new measurements of Fe-Mn interdiffusion in Fe- and Mn-rich garnet single crystals.

* Corresponding author.
E-mail address: zhangbaohua@zju.edu.cn (B. Zhang).

https://doi.org/10.1016/j.gsf.2023.101699

2. Experimental method and analyses

2.1. Sample preparation

Two natural aluminosilicate garnet single crystals sourced from the Putian area in Fujian Province, China were used as the starting material in this study. The major element analysis of garnet crystal was conducted using a Shimadzu EPMA 1720 electron probe at the Electron Probe Microanalysis Laboratory of Zhejiang University's School of Earth Sciences. The measurement conditions were as follows: acceleration voltage of 15 kV, current of 20 nA, beam spot diameter of 1 μm, and counting time of 30 s for each element (10 s for characteristic bands and 10 s for front and rear background each). Natural minerals and artificially synthesized oxides were used as standard samples, and the ZAF correction process was used to obtain the major elements content of garnet single crystal. Their chemical compositions were summarized in Table 1. The two crystals have similar Al and Si content, but substantial differences in their Mn and Fe contents, which can be expressed in terms of formula unit as $Sps_{92}Alm_6Grs_1$ and $Sps_{68}Alm_{29}Grs_2$ (Sps, Alm, and Grs denote $Mn_3Al_2Si_3O_{12}$-spessartine, $Fe_3Al_2Si_3O_{12}$-almandine, and $Ca_3Al_2Si_3O_{12}$-grossular, respectively). Retrieval of chemical formulas for these garnets from electron microprobe were based on 12 oxygen atoms in the desired formula, which involved converting units of quantity and normalizing the sums to conform to commonly used formulae conventions. Both crystals are inclusion-free and essentially homogeneous in major element concentrations.

The infrared (IR) spectra of the garnet crystals were obtained by Fourier-transformation infrared (FT-IR) spectroscopy using unpolarized light by a Jasco FTIR-6200 Equipper with an IRT-7000 infrared microscope. Optically clean and crack-free areas were selected for measurement, which was conducted in a continuous dry N_2 gas flow with an aperture size of 50 μm × 50 μm at 1 atm and 300 K. To ensure accuracy, more than five spectra were obtained for each crystal using unpolarized light. Water contents C_{H2O} in wt. ppm (parts per million by weight) were calibrated using the Beer-Lambert law $C_{H2O} = \Delta/(I \times t \times \gamma)$ (Bell et al., 1995), where Δ is the integrated hydrogen absorption bands in cm^{-2} with integration range chosen from 2800 to 3800 cm^{-1}, and t is the thickness in cm. The integral specific absorption coefficient I of 1.39 (Bell et al., 1995) in ppm^{-1} cm^{-2} was used, and an orientation factor γ of 1 (Paterson, 1982) was applied.

Table 1
Chemical compositions of starting garnet samples.

Oxides (wt.%)	Grt 1	Grt 2
K_2O	0.02	0.04
CaO	0.52	0.70
FeO	2.93	12.86
MnO	41.51	29.44
TiO_2	0.04	0.12
Cr_2O_3	0	0.02
Na_2O	0.03	0.07
MgO	0.02	0.07
Al_2O_3	21.16	20.15
SiO_2	33.77	35.51
Total	100.00	98.97
Sps (%)	92.05	68.24
Alm (%)	6.42	29.43
Grs (%)	1.45	2.06
Prp (%)	0.09	0.27
H_2O (ppm)	752	740

Sps, spessartine; Alm, almandine; Grs, grossular; Prp, pyrope.
Note that the H_2O content may have an error of up to 15%–20%.

2.2. High-pressure diffusion experiments

To prepare the diffusion couples for diffusion experiments, disks with approximately 1 mm diameter were cored from sliced pieces with a thickness of around 0.6–0.9 mm from the two garnet single crystals using ultrasonic drilling machine. One face of each disk was first polished using 0.25 μm diamond powder to achieve a smooth surface. Then, colloidal silica was used for further polishing. For each run, a diffusion couple was assembled using a pair of Mn-poor and Mn-rich garnet by closely contacting their polished surfaces. Fe capsule which was used, in order to effectively prevent the couple from absorbing water from surrounding materials (Irifune et al., 2016) and control the oxygen fugacity (fO_2) at a level close to the Fe-FeO (IW) buffer.

The interdiffusion experiments were performed at 6 GPa and 1273–1573 K utilizing a 18/11 multi-anvil cell assembly (Fig. 1). The experimental details are basically the same as our previous works (Zhang et al., 2019a, 2019b, 2021). The cell assembly was first compressed to 6 GPa and then heated to target temperature (up to 1673 K) at 100 K/min. The temperature was monitored by $W_{97}Re_3$-$W_{75}Re_{25}$ thermocouple, and no pressure effect on the emf was corrected. The fluctuation of temperature was within ± 10 K during the diffusion annealing. After maintaining the samples at the target temperature for a duration of 48 to 72 h, the power supply for heating was cut off and subsequently sample was decompressed slowly. The experimental conditions are summarized in Table 1. The pressure was calibrated using room temperature-phase transition of Bi (2.5 GPa and 7.7 GPa) and high temperature-transition of SiO_2 from quartz to coesite (Mirwald and Massonne, 1980).

2.3. Profile analysis and diffusion coefficient determination

Each recovered interdiffusion couple was cut into two halves perpendicular to the contact interface. One half was prepared for FTIR measurement to determine the water content after diffusion. Before measurement, this half was double-polished and dried at ~ 473 K in a vacuum oven for 24 h to remove any surface absorbed water. The other half was polished with diamond powders and colloidal silica for the next series of analyses. The recovered samples remain as garnet confirmed by X-ray diffraction, without other phases. To obtain Fe–Mn concentration profiles and element mapping of diffusion couples, a 1-μm beam accelerated by a voltage of 15 kV and a current of 12 nA was adopted using a Shimadzu EPMA 1720 electron microprobe (EPMA). With 1.25 μm set as the step size, more than two diffusion profiles were acquired for each couple across the contact interface.

Two garnet single crystals are rich in spessartine and almandine (Table 1), one of which is nearly an end-member composition. Manganese and iron are the most abundant, and their concentration gradient is dominant. The concentrations of all other components are very similar in both garnets. In this case, the diffusion of Manganese and iron can be treated as effective binary diffusion (EBD) or pseudobinary interdiffusion (Zhang, 2010).

A method for determining the Fe/Mn content-dependent interdiffusion coefficient for a binary or pseudobinary couple is the Boltzmann-Matano method (Matano, 1933; Crank, 1975). The measured concentration profiles were first iterated to the sigmoidal function below:

$$C(x) = A_0\left(1 - \frac{1}{(1+\exp(A_1x + A_2))^{A_3}}\right) + A_4 \quad (1)$$

where $C(x)$ is the Fe/Mn concentration as a function of perpendicular distance x from the initial contact interface), and A_0, A_1, A_2, A_3, and A_4 are fitting parameters. Then, the Matano interface

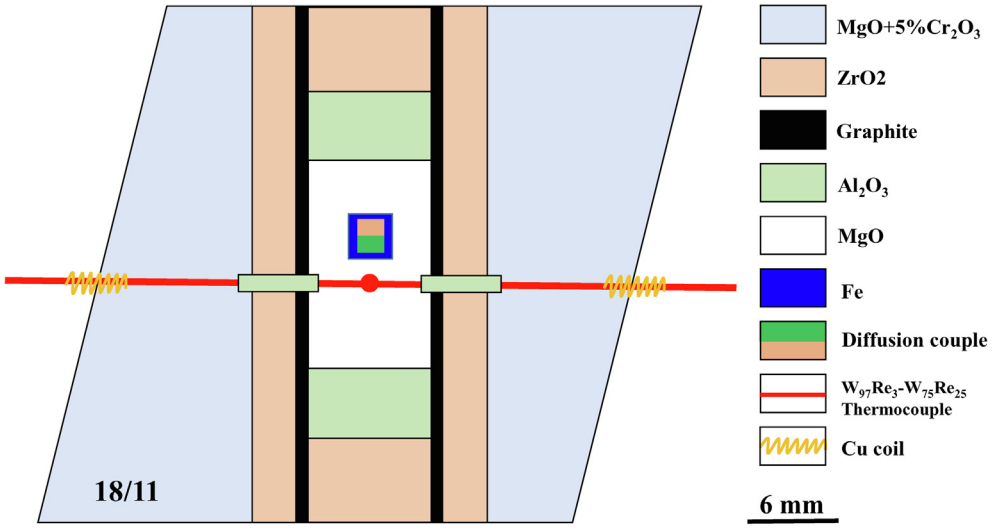

Fig. 1. Cell assemblage for the high pressure diffusion experiments in a Kawai-type multi-anvil apparatus.

(where $x = 0$) was found by integrating across the profile until the following condition was satisfied:

$$\int_{C_1}^{C_2} x\mathrm{d}C = 0 \tag{2}$$

where C_1 and C_2 are the maximum and minimum concentrations respectively in the diffusion profiles. Finally, the concentration-dependent interdiffusion coefficient was obtain by equation below:

$$D(C^*) = -\frac{1}{2t}\left(\frac{\mathrm{d}x}{\mathrm{d}C}\right)_{C^*}\int_{C_1}^{C^*} x\mathrm{d}C \tag{3}$$

where t is the annealing duration and $D(C^*)$ is the concentration-dependent interdiffusion coefficient at concentration of C^*. The integral part in Eq. (3) was obtained by counting squares xdC. The gradient $(dx/dC)_{C^*}$ was the first derivative of the profile at concentration of C^*. The error estimated from propagated uncertainty was negligibly small.

3. Results

Fig. 2 exhibits examples of FTIR spectra for Mn-rich garnet before and after diffusion annealing. No change in OH speciation and obvious water loss are found during annealing (Table 1 and Fig. 2). Two absorption peaks at 3579 and 3622 cm^{-1} were observed, which are similar to previous study (Zhang et al., 2019a). A representative back-scattered electron image of a cross-section from a diffusion couple (run 1 K034), which was annealed at 6 GPa and 1573 K for 48 h, is shown in Fig. 3a. Horizontal cracks were probably caused by quench or decompression. Such cracks are expected to close during the diffusion annealing at high temperatures. Element mappings of Si, Fe and Mn on the area are demonstrated in Fig. 3b–d. Clearly, the Si concentration is homogeneous in both the Mn-poor and -rich garnets (Fig. 3b), while the Mn and Fe concentration gradients in the Mn-rich end are much larger than those on the Fe-rich end (Fig. 3c and d). The imperfect interface of the diffusion couples is likely a consequence of nonuniform volume (or surface) changes of the samples at high pressure and temperature.

Fig. 4 illustrates typical diffusion profile from EMPA measurements and fitting lines from the Boltzmann–Matano analyses. The Matano interface for each diffusion couple is nearly the same as their initial contact interfaces (Fig. 4a). The diffusion profile is asymmetric, which suggests a composition-dependent diffusion coefficient. Meanwhile, the profiles (~15–40 μm) are long enough to avoid correct for convolution of the true concentration profiles due to the spatial averaging effect in the microprobe spot analysis (Ganguly et al., 1988).

The Fe-Mn interdiffusion coefficient ($D_{Fe\text{-}Mn}$) decreases slightly with increasing Fe content (X_{Fe}) (or decreasing Mn content) (Fig. 4b). On the contrary, Elphick et al. (1985) indicated that $D_{Fe\text{-}Mn}$ increases with increasing Fe content (X_{Fe}). This difference could be attributed to the composition and water content of diffusion couples. Ganguly et al. (1988) revealed that the self-diffusion coefficient of Fe (D_{Fe}) and Mn (D_{Mn}) significantly decreases as the Mn content decreases in diffusion couples. Our diffusion couples (Sps-Sps) contain quite more manganese (Mn) than the diffusion couples (Sps-Alm) of Elphick et al. (1985). This increasing Mn may change the dimension of the eight-coordinated site or the unit-cell volume of the garnet, thus causing the negative compositional dependence to X_{Fe} in our study. Additionally, Elphick et al.

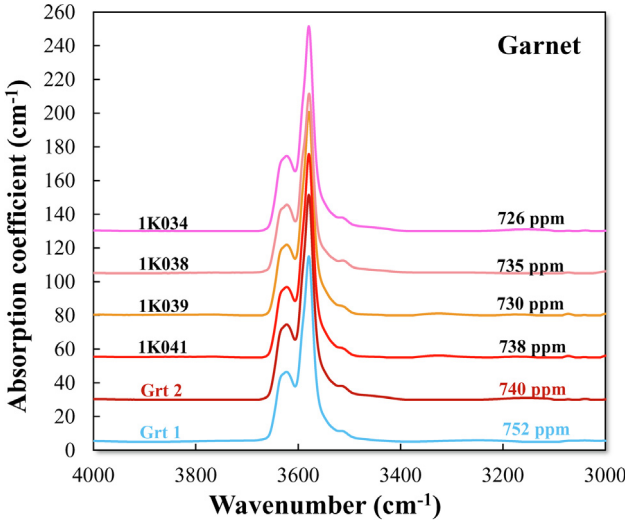

Fig. 2. Unpolarized FT-IR spectra obtained in the Mn-rich garnet samples before and after diffusion annealing. Grt 1 and Grt 2 represent the starting samples for Mn-rich garnet before diffusion (Table 1). Note that the C_{H2O} before and after diffusion are essentially the same, which may have an error of up to 15%–20%.

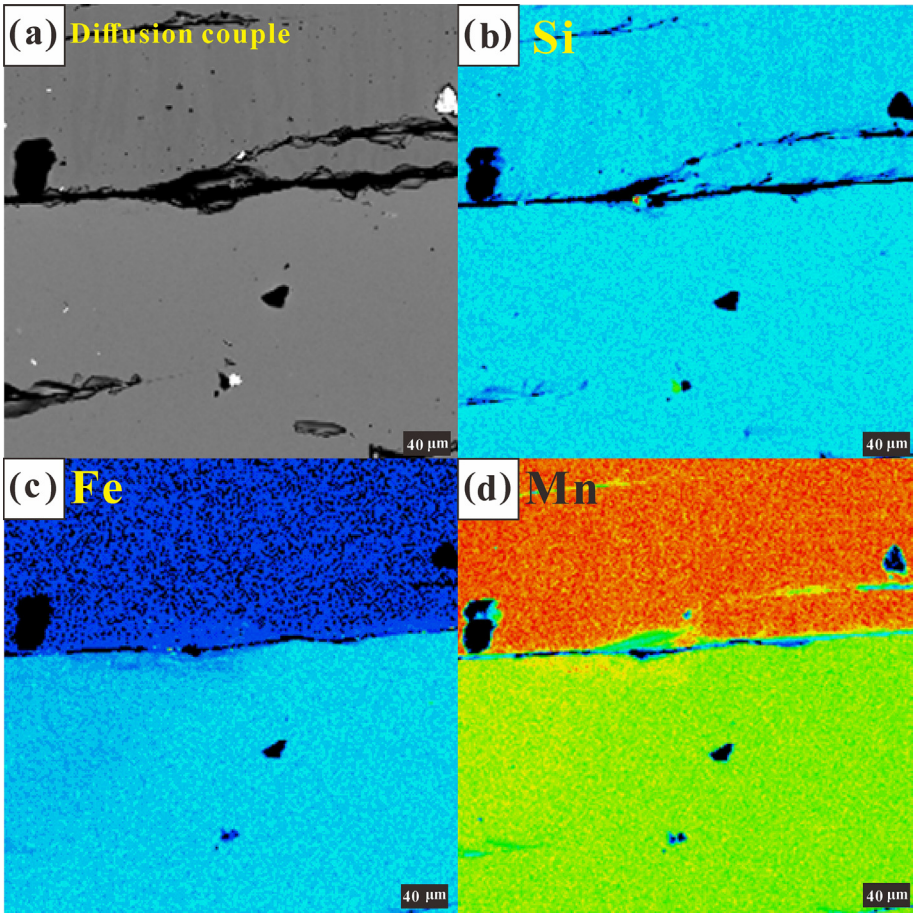

Fig. 3. (a) Backscattered electron image of the recovered sample (1 K034) annealing at 1573 K for 48 h. Elements map of silicon (b), iron (c) and manganese (d) for the same area in (a).

(1985) found that the Fe-Mg interdiffusion coefficient ($D_{Fe\text{-}Mg}$) increases with increasing X_{Fe} in Alm-Pyr diffusion couples. However, Zhang et al. (2019b) showed that $D_{Fe\text{-}Mg}$ is nearly independent of X_{Fe}, whose diffusion couples (Alm-Pyr) contained more water than the former. As is well known, the incorporation of hydrogen can alter the structure and physical properties of nominally anhydrous minerals including garnet. As a result, the incorporation of water into garnet may impact the Fe or Mn dependence on $D_{Fe\text{-}Mn}$. More importantly, the effects of water and composition on $D_{Fe\text{-}Mn}$ require further systematic and quantitative investigation to gain a deeper understanding of these relationships.

Considering the negative compositional dependence, Fe–Mn interdiffusion coefficients in garnet measured in our work were fitted to the equation below (Yamazaki and Irifune, 2003; Zhang et al., 2019a, 2019b, 2021):

$$D_{Fe-Mn}(m^2/s) = D_0 X_{Fe}^n \exp(-E^*/RT) \quad (4)$$

where D_0 is the pre-exponential factor, E is the activation enthalpy, X_{Fe} is the iron concentration, n is a constant, R is the ideal gas constant, and T is the absolute temperature. Activation energy is assumed to be linearly dependent on iron concentration as follows:

$$E^* = (1 - X_{Fe})E^*_{Mn} + X_{Fe}E^*_{Fe} \quad (5)$$

A global fit of all data gives $D_0 = 8.06^{+9.87}_{-6.04} \times 10^{-9}$ m^2/s, $E^*_{Mn} = 248 \pm 27$ kJ/mol, $E^*_{Fe} = 226 \pm 59$ kJ/mol, $n = -1.36 \pm 0.51$. The errors were mainly derived from the uncertainties associated with EPMA measurement, the Boltzmann–Matano analysis, and the least-squares fitting to Eq. (4). Fig. 5 shows the temperature dependence of Fe-Mn interdiffusion coefficient at X_{Mn} = 0.79 for Mn-bearing garnet with 750 ppm H_2O. The activation energy E can be determined from the slope of the best-fit line to Eq. (4). Since the water contents in different samples are essentially the same, and there is no water loss during diffusion annealing (Fig. 2 and Table 2), it is unnecessary to consider the water effect in the overall fitting of the experimental data in this study.

4. Discussion

4.1. Comparison with previous studies

To know the rate-controlling mechanism in garnet, our Fe-Mn interdiffusivities are compared with those of various cations (Fe-Mg, Fe, Mg, Mn) (Elphick et al., 1985; Chakraborty and Ganguly, 1992; Borinski et al., 2012; Zhang et al., 2019a) in Fig. 6. It is found that the Fe-Mn interdiffusion coefficients determined in this study, under hydrous conditions, are faster than the Fe-Mn interdiffusion coefficients reported by Elphick et al. (1985) at least 1.5 log units, and also faster than the Mg, Mn and Fe diffusivities in either Mn-rich garnet (Chakraborty and Ganguly, 1992) or Fe-Mg garnet (Borinski et al., 2012). However, our determined Fe-Mn interdiffusivities are comparable to the Fe-Mg interdiffusivities obtained by Zhang et al. (2019a) with 100 wt ppm H_2O. At the same time, the Fe-Mn interdiffusivities reported by Elphick et al. (1985) are similar to the Fe-Mg interdiffusivities in anhydrous garnet obtained by Zhang et al. (2019a).

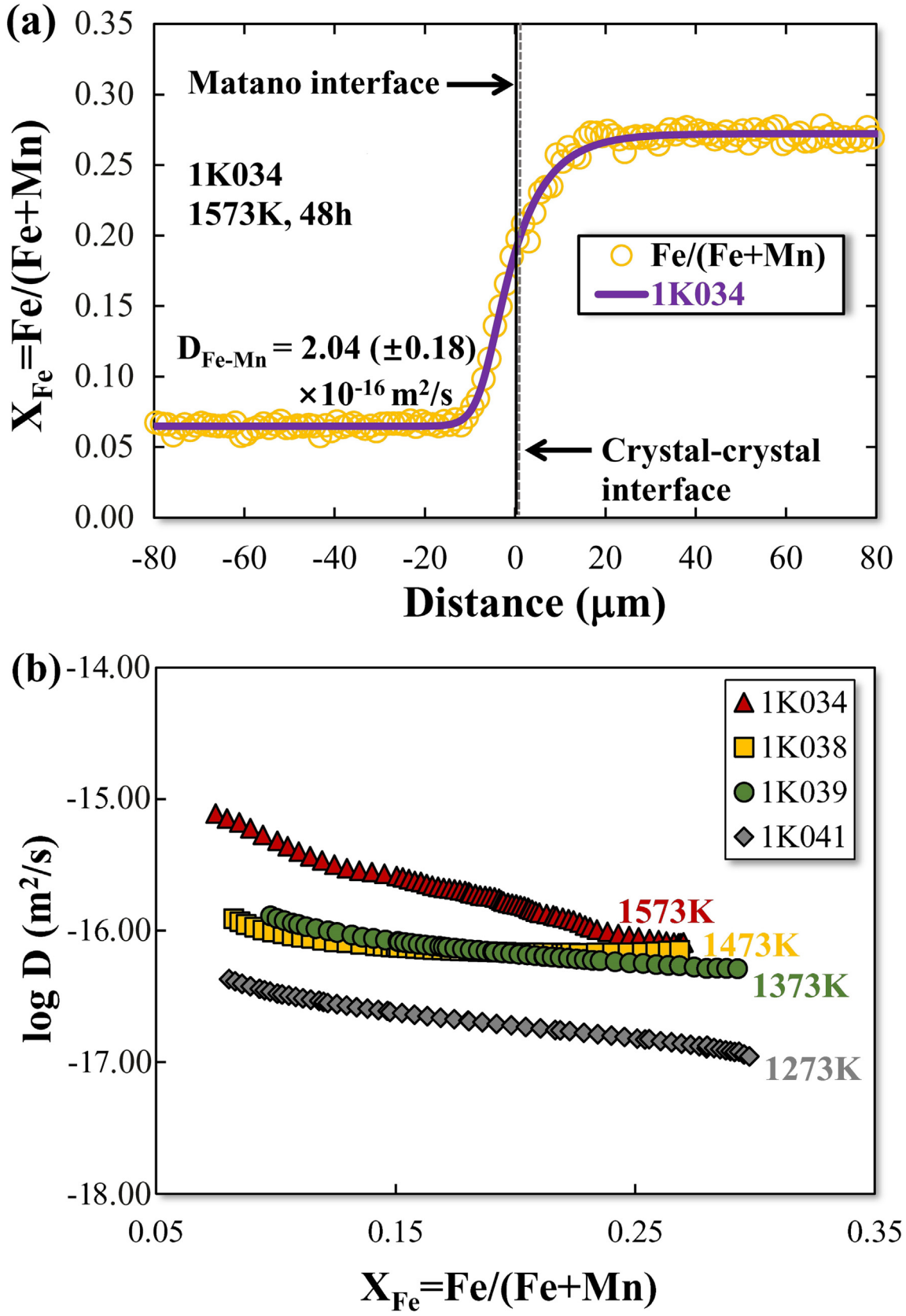

Fig. 4. (a) Representative Fe–Mn interdiffusion profile in run 1 K034 (1573 K for 48 h). The Matano interface is set at x = 0. The solid line shows the Boltzmann-Matano analysis by Eq. (1). (b) Fe-Mn interdiffusion coefficient at different temperatures as a function of iron content. A small negative iron-content dependence is observed.

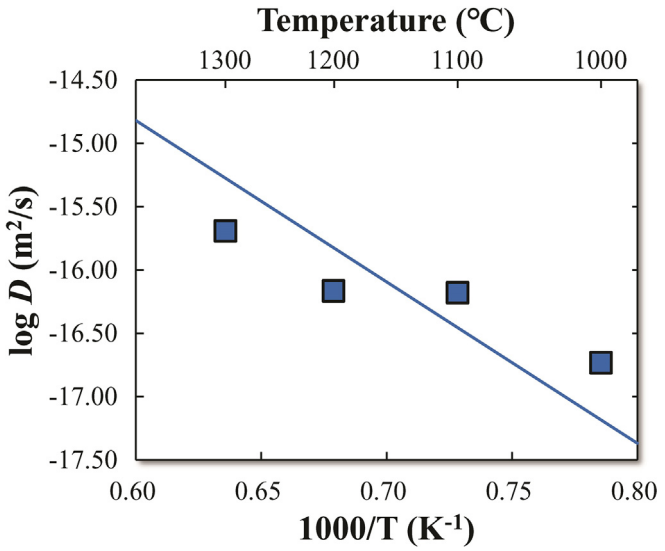

Fig. 5. Experimentally measured Fe-Mn interdiffusion coefficient in garnet at X_{Mn} = 0.79 as a function of reciprocal temperature.

Recently, Zhang et al. (2019a) demonstrated a large water effect on D_{Fe-Mg} in garnet by investigating the influence of water on kinetics of Fe-Mg interdiffusion, using diffusion couples of pyrope and almandine aggregates with water content (C_{H2O}) ranging from < 7 up to 1260 ppm at 3 GPa and 1373–1673 K. As shown in Fig. 6, Fe-Mg interdiffusion in garnet with even ~100 ppm H_2O is faster than that in anhydrous sample by two orders of magnitude. Consequently, the faster Fe-Mn interdiffusivities obtained in this study may be caused by the presence of a large amount of water in garnets (~750 wt ppm), despite previous works not measuring the specific water content in their garnets. Although the oxygen fugacity in the present study (~IW buffer) is lower than that (graphite buffer) in the experiment of Elphick et al. (1985), it is found that the oxygen fugacity only has a tiny effect on defect concentrations and, eventually, on the diffusion mechanism in garnet (Zhang et al., 2019a). Thus, our faster Fe-Mn interdiffusion rates are hard to be explained by variation of oxygen fugacity. Moreover, the activation energy for Fe-Mn interdiffusion in garnet (~244 kJ/mol at X_{Mn} = 0.79) is comparable to previously determined values (239–284 kJ/mol for D_{Fe-Mg}, D_{Mg}, D_{Fe} and D_{Mn}) (Elphick et al., 1985; Chakraborty and Ganguly, 1992; Borinski et al., 2012; Zhang et al., 2019a).

Table 2
A summary of experimental conditions and results of Fe-Mn interdiffusion coefficients in garnet at 6 GPa.

Run no.	T (K)	Time (h)	Capsule	D_{Fe-Mn} (m^2/s)	
				X_{Mn} = 0.79[a]	X_{Mn} = 0.82[b]
1 K034	1573	48	MgO + Fe	2.05 (0.21) × 10^{-16}	1.52 (0.11) × 10^{-16}
1 K038	1473	48	MgO + Fe	6.82 (0.05) × 10^{-17}	7.11 (0.12) × 10^{-17}
1 K039	1373	56	MgO + Fe	6.60 (0.23) × 10^{-17}	7.42 (0.27) × 10^{-17}
1 K041	1273	72	MgO + Fe	1.84 (0.08) × 10^{-17}	2.12 (0.09) × 10^{-17}

[a] The average of D_{Fe-Mn} between X_{Mn} = 0.78 and X_{Mn} = 0.80. The range of uncertainties is given in parentheses.
[b] The average of D_{Fe-Mn} between X_{Mn} = 0.81 and X_{Mn} = 0.83. The range of uncertainties is given in parentheses.

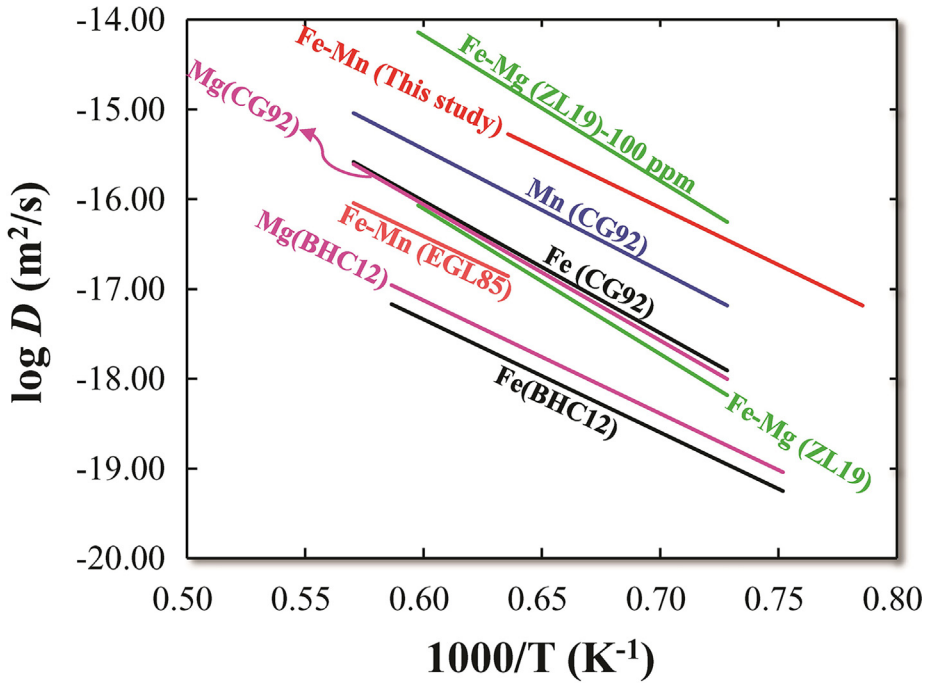

Fig. 6. A comparison of cation diffusion coefficients in garnet reported in different studies. Data source: CG92 (Chakraborty and Ganguly, 1992) (these data were combined with those of Loomis et al., 1985), EGL85 (Elphick et al., 1985), BHC12 (Borinski et al., 2012) (these data based on results from Ganguly et al., 1998), ZL19 (Zhang et al., 2019a).

4.2. Geological implications

Diffusion kinetic modeling on compositional zoning in garnet due to major elements provide important constraints on chemical equilibrium for mineral phases and the timescales of metamorphic processes, including heating and cooling rates, which indicate the burial and exhumation rates, respectively (Ganguly et al., 2000; Ganguly, 2002; Baxter and Scherer, 2013; Zhang, 2017; Li et al., 2018). In particular, the diffusion coefficient is a critical parameter for theoretical simulations of those complex physical and chemical processes.

Since cations (Fe-Mn/Mg, Fe, Mn, etc.) are the fastest diffusing species in garnet, we can use Fe-Mn diffusion data to estimate the duration of a metamorphic event from the homogenization extent of zoned garnets. By considering the mean diffusional length to be $d = (4Dt)^{1/2}$ (Crank, 1975), where d is the radius of a garnet, the time t required for homogenization of a garnet zoning at a given temperature would depend on the diffusion coefficient D. As a result, our experiments were carried out under more reduced conditions than those of Elphick et al. (1985). Fig. 7 shows the time required for the compositional homogenization of an initially zoned garnet with various diameter at a given temperature of 800 °C. Since the rates of Fe-Mn diffusion in hydrous garnet obtained in this study are higher than those of anhydrous garnet in Elphick et al. (1985) by three orders of magnitude, the diffusion adjustment of the composition distribution may take much less time than previously thought (Schwandt et al., 1995). For example, in the present study, the time required for chemical homogenization of garnet crystals with a diameter of 6 mm at 800 °C is about 10^5 years, which is significantly shorter than that based on Elphick et al. (1985) (~10^8 years) (Fig. 7). Therefore, Fe-Mn diffusion in garnet may play a significant role during the formation of compositional zoning in amphibolite grade garnet. Especially, the role of water in modeling the metamorphic processes should be taken into account.

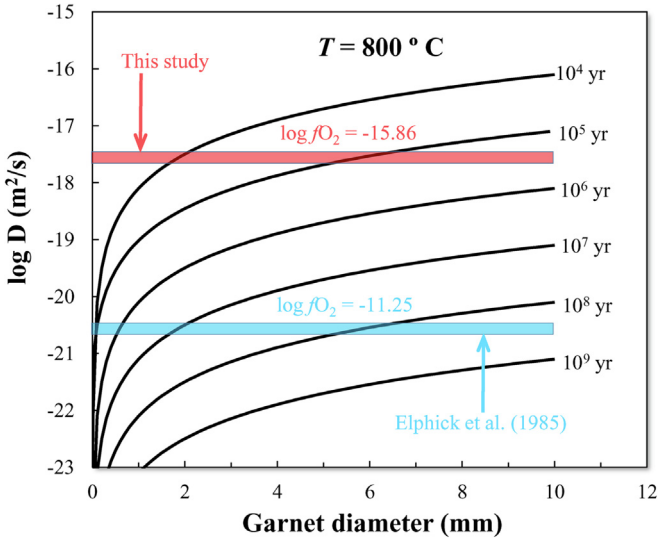

Fig. 7. The time required for chemical homogenization of an initially zoned garnet as a function of its diameter. Black solid lines represent the approximate time required for chemical homogenization of a garnet at 800 °C on the basis of a mean distance of diffusion. The light blue and red rectangles indicate the values of $D_{Fe\text{-}Mn}$ reported by Elphick et al. (1985) and this study, respectively, the width of the shaded region represents the uncertainty of the log$D$ values. The oxygen fugacity (fO_2) was roughly estimated according to the methods of Frost (1991) and O'Neill and Pownceby (1993). (For interpretation of the references to colour in this figure legend, the reader is referred to the web version of this article.)

5. Conclusions

The temperature dependence of Fe-Mn interdiffusion coefficient was investigated in hydrous natural single crystals of Mn-bearing garnet at 6 GPa and 1273–1573 K using the diffusion couple method. The experimental results demonstrate that the $D_{Fe\text{-}Mn}$ decreases slightly with increasing Fe content (X_{Fe}). This negative compositional dependence is contrary to previous observations in other minerals such as olivine, wadsleyite, and ringwoodite, where the interdiffusion coefficient typically shows a positive dependence on composition. Comparison among available all diffusivities of various cations (Fe-Mn/Mg, Mg, Fe, Mn) in garnet shows that water (i.e., OH) may strongly accelerate the ionic diffusion. The role of water in modeling chemical homogenization of the compositional zoning for metamorphic processes may be much larger than previously considered, indicating a much shorter time required for the chemical equilibrium.

CRediT authorship contribution statement

Yanjun Yin: Formal analysis, Investigation, Methodology, Writing – original draft. **Baohua Zhang:** Conceptualization, Data curation, Formal analysis, Funding acquisition, Methodology, Project administration, Resources, Supervision, Validation, Writing – review & editing. **Xinzhuan Guo:** Supervision, Writing – review & editing.

Declaration of Competing Interest

The authors declare that they have no known competing financial interests or personal relationships that could have appeared to influence the work reported in this paper.

Acknowledgments

We thank Suwen Qiu for assistance with electron microprobe measurements at Zhejiang University and Drs. H. Fei and C. Zhao for reading the draft. This study was financially supported by the National Natural Science Foundation of China (41973056, 41773056) and Key Research Program of Frontier Sciences of CAS (ZDBS-LY-DQC015) to B. Zhang, and the Fundamental Research Funds for the Central Universities (K20210168). Data presented as part of this study are available from Zenodo (https://doi.org/10.5281/zenodo.7080353).

References

Baxter, E.F., Scherer, E.E., 2013. Garnet Geochronology: Timekeeper of Tectonometamorphic Processes. Elements 9, 433–438. https://doi.org/10.2113/gselements.9.6.433.

Bell, D.R., Ihinger, P.D., Rossman, G.R., 1995. Quantitative analysis of trace OH in garnet and pyroxenes. Am. Mineral. 80, 465–474. https://doi.org/10.2138/am-1995-5-607.

Borinski, S.A., Hoppe, U., Chakraborty, S., Ganguly, J., Bhowmik, S.K., 2012. Multicomponent diffusion in garnets I: general theoretical considerations and experimental data for Fe-Mg systems. Contrib. Miner. Petrol. 164, 571–586. https://doi.org/10.1007/s00410-012-0758-0.

Chakraborty, S., Ganguly, J., 1991. Compositional zoning and cation diffusion in garnets. In: Ganguly, J. (Ed.), Diffusion, Atomic Ordering, and Mass Transport: Selected Topics in Geochemistry. Springer US, New York, NY, pp. 120–175. https://doi.org/10.1007/978-1-4613-9019-0_4.

Chakraborty, S., Ganguly, J., 1992. Cation diffusion in aluminosilicate garnets: experimental determination in spessartine-almandine diffusion couples, evaluation of effective binary diffusion coefficients, and applications. Contrib. Miner. Petrol. 111, 74–86. https://doi.org/10.1007/BF00296579.

Crank, J., 1975. The Mathematics of Diffusion (2nd ed.). Oxford University Press, London, pp. 1–414.

Creighton, S., 2009. A semi-empirical manganese-in-garnet single crystal thermometer. Lithos 112, 177–182. https://doi.org/10.1016/j.lithos.2009.05.011.

Elphick, S.C., Ganguly, J., Loomis, T.P., 1985. Experimental determination of cation diffusivities in aluminosilicate garnets. Contrib. Miner. Petrol. 90, 36–44. https://doi.org/10.1007/BF00373040.

Frost, B.R., 1991. Introduction to oxygen fugacity and its petrologic importance. Rev. Mineral. Geochem. 25, 1–9. https://doi.org/10.1515/9781501508684-004.

Ganguly, J., 2002. Diffusion kinetics in minerals: principles and applications to tectono-metamophic processes. EMU Notes Mineral. 4, 271–309. https://doi.org/10.1180/EMU-notes.4.9.

Ganguly, J., Bhattacharya, A., Chakraborty, S., 1988. Convolution effect in the determination of compositional profiles and diffusion coefficients by microprobe step scans. Am. Mineral. 73, 901–909.

Ganguly, J., Cheng, W., Chakraborty, S., 1998. Cation diffusion in aluminosilicate garnets: experimental determination in pyrope-almandine diffusion couples. Contrib. Miner. Petrol. 131, 171–180. https://doi.org/10.1007/s004100050386.

Ganguly, J., Dasgupta, S., Cheng, W., Neogi, S., 2000. Exhumation history of a section of the Sikkim Himalayas, India: records in the metamorphic mineral equilibria and compositional zoning of garnet. Earth Planet. Sci. Lett. 183, 471–486. https://doi.org/10.1016/S0012-821X(00)00280-6.

Irifune, T., Kawakami, K., Arimoto, T., Ohfuji, H., Kunimoto, T., Shinmei, T., 2016. Pressure-induced nano-crystallization of silicate garnets from glass. Nat. Commun. 7, 13753. https://doi.org/10.1038/ncomms13753.

Li, B., Ge, J., Zhang, B., 2018. Diffusion in garnet: a review. Acta Geochim. 37, 19–31. https://doi.org/10.1007/s11631-017-0187-x.

Loomis, T.P., 1983. Compositional Zoning of Crystals: A Record of Growth and Reaction History. In: Saxena, S.K. (Ed.), Kinetics and Equilibrium in Mineral Reactions. Springer, New York, pp. 1–60.

Loomis, T.P., Ganguly, J., Elphick, S.C., 1985. Experimental determination of cation diffusivities in aluminosilicate garnets. Contrib. Miner. Petrol. 90, 45–51. https://doi.org/10.1007/BF00373040.

Matano, C., 1933. On the relation between the diffusion-coefficients and concentrations of solid metals. Jap. J. Phys. 8, 109–113.

Mirwald, P.W., Massonne, H.J., 1980. The low-high quartz and quartz-coesite transition to 40 kbar between 600°C and 1600°C and some reconnaissance data on the effect of $NaAlO_2$ component on the low quartz-coesite transition. J. Geophys. Res.: Solid Earth 85, 6983–6990. https://doi.org/10.1029/JB085iB12p06983.

O'Neill, H.S.C., Pownceby, M.I., 1993. Thermodynamic data from redox reactions at high temperatures. I. An experimental and theoretical assessment of the electrochemical method using stabilized zirconia electrolytes, with revised values for the Fe- "FeO", Co-CoO, Ni-NiO and Cu-Cu_2O oxygen buffers, and new data for the W-WO_2 buffer. Contrib. Miner. Petrol. 114, 296–314. https://doi.org/10.1007/BF01046533.

Paterson, M.S., 1982. The determination of hydroxyl by infrared absorption in quartz, silicate glasses and similar materials. Bull. Minéral. 105, 20–29.

Perchuk, A.L., Burchard, M., Schertl, H.P., Maresch, W.V., Gerya, T.V., Bernhardt, H.J., Vidal, O., 2008. Diffusion of divalent cations in garnet: multi-couple experiments. Contrib. Miner. Petrol. 157, 573–592. https://doi.org/10.1007/s00410-008-0353-6.

Schwandt, C.S., Cygan, R.T., Westrich, H.R., 1995. Mg self-diffusion in pyrope garnet. Am. Mineral. 80, 483–490. https://doi.org/10.2138/am-1995-5-609.

Yamazaki, D., Irifune, T., 2003. Fe–Mg interdiffusion in magnesiowüstite up to 35 GPa. Earth Planet. Sci. Lett. 216, 301–311. https://doi.org/10.1016/S0012-821X(03)00534-X.

Zhang, Y., 2010. Diffusion in minerals and melts: Theoretical background. Rev. Mineral. Geochem. 72, 5–59. https://doi.org/10.2138/rmg.2010.72.2.

Zhang, B., 2017. An overview of Fe–Mg interdiffusion in mantle minerals. Sur. Geophys. 38, 727–755. https://doi.org/10.1007/s10712-017-9415-5.

Zhang, B., Li, B., Zhao, C., Yang, X., 2019a. Large effect of water on Fe–Mg interdiffusion in garnet. Earth Planet. Sci. Lett. 505, 20–29. https://doi.org/10.1016/j.epsl.2018.10.015.

Zhang, B., Yoshino, T., Zhao, C., 2019b. The effect of water on Fe–Mg interdiffusion rates in ringwoodite and implications for the electrical conductivity in the mantle transition zone. J. Geophys. Res.: Solid Earth 124, 2510–2524. https://doi.org/10.1029/2018JB016415.

Zhang, B., Zhao, C., Yoshino, T., 2021. Fe–Mg interdiffusion in wadsleyite and implications for water content of the transition zone. Earth Planet. Sci. Lett. 554, 116672. https://doi.org/10.1016/j.epsl.2020.116672.